ChemComm

RSC Publishing

COMMUNICATION

View Article Online
View Journal | View Issue

Facile synthesis of Au–Ag core–shell nanoparticles with uniform sub-2.5 nm interior nanogaps†

Cite this: *Chem. Commun.*, 2013, **49**, 8519

Received 10th May 2013,
Accepted 25th July 2013

DOI: 10.1039/c3cc43523g

www.rsc.org/chemcomm

Zhong Zhang, Sha Zhang and Mengshi Lin*

A facile method was established to fabricate uniform nanogaps between a Au core and a Au–Ag alloy shell. The size of nanogaps is controllable due to fast dissolution of AgCl and AgBr in CTAB and the crystal growth of the shell on a designed template. These Au–Ag core–shell nanoparticles with uniform sub-2.5 nm interior nanogaps can be potentially used for various applications.

Gold and silver nanoparticles (NPs) have been increasingly used in many areas due to their versatility in surface modifications and tunable optical properties. For example, Au NPs have been employed for cancer diagnosis and therapy, drug delivery, and DNA identification.[1] The localized surface plasmon resonance (LSPR) on noble metal NPs, such as Au or Ag NPs, makes them ideal substrates for various applications.[2]

It is now well understood that the nanosized gap junction between noble metal NPs could induce enormous electromagnetic field that enhances the Raman signals of the tested samples.[3] However, most surface enhanced Raman substrates suffer from poor reproducibility mainly due to non-uniform nanostructures. A novel approach to solve this problem is to create uniform nanosized gaps between Au or Ag nanostructures. For example, salt and DNA have been used to induce the aggregation of NPs, thus leading to the formation of nanosized gap junctions.[4] However, the aggregation of NPs is difficult to control, leading to inconsistent gap distances and non-uniform gap topography.[3c,5] Due to high demand for nanoparticles with uniform nanogaps, a method using conventional lithography has been proposed to fabricate sub-10 nm metallic nanogap arrays with precise control of the gap size, position, shape, and orientation.[6] Unfortunately, it is still very difficult to synthesize 1.0–2.5 nm nanogaps by conventional lithography technology. A new class of nanostructures with well-defined 1.2 nm interior nanogaps has been synthesized by coating a gold shell on a gold nanosphere which was previously modified with thiolated ssDNA.[5a] However, it is a complex and expensive route to modify a large scale of gold NPs with thiolated ssDNA. The size of the gap between the core and the shell could not be controlled. It remains a great challenge to fabricate a large scale of nanogaps with uniform gap distance, and more importantly, with controllable sizes of less than 2.5 nm without using thiolated ssDNA.

Herein, we report a facile method for synthesizing Au–Ag core–shell NPs with uniform hollow interior nanogaps between Au cores and Au–Ag alloy shells. As shown in Scheme 1, spherical Au NPs (*ca.* 28.9 ± 3.4 nm in diameter) were prepared by the citrate reduction method.[7] A thin layer of Ag shell was then deposited on the as-prepared Au NPs by reducing silver nitrate in the presence of ascorbic acid. The reaction occurred at room temperature and used Au NPs as seeds to grow the silver shell (Fig. S1, ESI†).[8] The Au–Ag core–shell NPs were then directly mixed with cetyltrimethylammonium bromide (CTAB) solution without any purification, followed by the addition of $HAuCl_4$ solution. Using the Ag shell as a sacrificial template, the galvanic reaction between $AuCl_4^-$ and Ag initiated on the surface of the Ag shell, oxidizing Ag to Ag^+ and resulting in the formation of AgCl and AgBr. Fortunately, the CTAB can solubilize AgCl and AgBr formed upon the oxidation of the silver shell, thus avoiding the crystalline growth of AgCl and AgBr.[9] In the meantime, the Au atoms were produced upon the galvanic reaction and nucleated on the surface of the Ag shell.[10] Due to the presence of ascorbic acid, Ag^+ was reduced and alloyed with Au atoms to form a Au–Ag alloy shell. The stoichiometric relationship of $AuCl_4^-$ and Ag is 1 to 3 for the galvanic reaction.

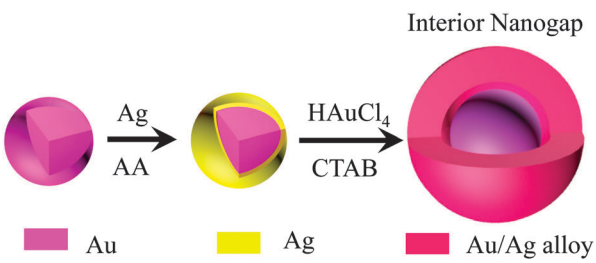

Scheme 1 Fabrication of uniform interior nanogaps by Au–Ag core–shell NPs through controlled galvanic reaction between $HAuCl_4$ and the Ag shell.

Division of Food Systems & Bioengineering, University of Missouri, Columbia, MO, USA 65211-5160. E-mail: linme@missouri.edu; Fax: +1 57 3884 7964; Tel: +1 57 3884 7964

† Electronic supplementary information (ESI) available: Synthetic procedures and characterization methods, TEM and Uv-vis data. See DOI: 10.1039/c3cc43523g

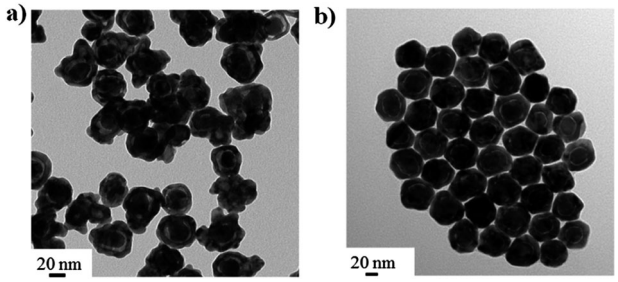

Fig. 1 TEM images of NPs obtained by mixing Au–Ag core–shell NPs (500 μL) with $HAuCl_4$ (1.0 mM, 500 μL): (a) without CTAB and (b) with CTAB (0.1 M, 500 μL).

Therefore, a hollow space was formed between the Au core and the Au–Ag alloy shell using the Ag shell as a sacrificial template. If the average thickness of the Ag shell was controlled to less than ~3.3 nm, hollow nanogaps would be fabricated between the Au core and the Au–Ag alloy shell. More importantly, the size of nanogaps could also be controlled by adjusting the thickness of the Ag template.

The effect of surfactants and complexing agents on the formation of interior nanogaps was examined. Fig. 1 shows the TEM images of NPs fabricated with and without CTAB. Without CTAB, $AuCl_4^-$ oxidized Ag to Ag^+ and turned Ag^+ into insoluble AgCl once $HAuCl_4$ was added into the solution of Au–Ag core–shell NPs. Due to the insolubility of AgCl in aqueous solution, AgCl migrated from the surface of the Au core to the solution and precipitated. Meanwhile, excess $HAuCl_4$ was continuously reduced by the galvanic reaction and ascorbic acid, resulting in the formation of crystals with irregular shapes because of the interference from insoluble AgCl. Instead of forming a nanogap between the core and the shell, the NPs expanded and formed a big gap (5–15 nm) between the core and the shell as shown in Fig. 1a. It is also clearly shown that these big gaps were filled with a low density of crystals. In contrast, a hollow nanogap was formed between the Au core and the Au–Ag alloy shell when sufficient CTAB was used (Fig. 1b). In the galvanic reaction, the oxidized Ag^+ would not form a precipitate with Cl^- and Br^- in the presence of CTAB due to high solubility of AgCl and AgBr in CTAB solution. The results of the control indicate that AgCl and AgBr could completely dissolve in CTAB solution when the molar ratio of Ag to CTAB was lower than 1 : 75 (Fig. S2, ESI†). Without the interference from insoluble AgCl and AgBr, the galvanic reaction allows the formation of a uniform nanogap using the Ag shell as a template. Because of the use of a large amount of ascorbic acid as a reducing agent and a low mismatch of Au and Ag lattices (0.1%), a crystalline alloy shell of Au–Ag was thus formed outside the nanogap. Distinct LSPR was observed for the Au–Ag core–shell NPs after reacting with $HAuCl_4$ in aqueous solution and in CTAB solution (Fig. S3, ESI†). With CTAB, the product has similar LSPR spectral patterns to those of Au NPs; while without CTAB, the LSPR spectra of products have a wide shoulder extending from 514 to 700 nm that was contributed by the Au core and the shell, indicating that huge hollow space was formed between the core and the shell.[10] Therefore, it is important to keep CTAB in a sufficient concentration to solubilize AgCl and AgBr. If the supply of CTAB is insufficient, AgCl and AgBr could not totally dissolve in solution and thus disturbed the formation of nanogaps and the Au–Ag alloy shell. Larger nanogaps and shells with irregular shapes were detected when the supply of CTAB was insufficient (Fig. S4a, ESI†). When CTAB was

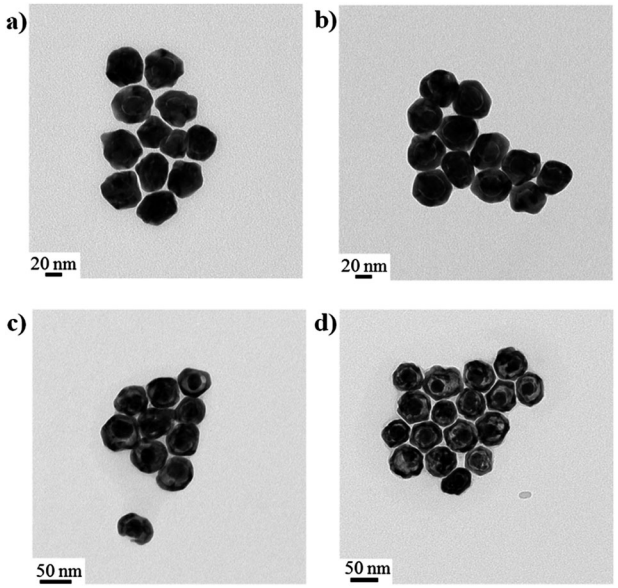

Fig. 2 TEM images of NPs obtained by mixing Au–Ag core–shell NPs (500 μL) with $HAuCl_4$ (1.0 mM, 500 μL) in the presence of CTAB (0.1 M, 500 μL). Ag coating: (a) 0.5 mM, (b) 1.0 mM, (c) 2.0 mM and (d) 3.0 mM $AgNO_3$ reduced by ascorbic acid.

substituted by ammonia hydroxide, solid Au NPs without nanogaps were produced (Fig. S4b, ESI†). This phenomenon indicates that CTAB promotes the formation of nanogaps by binding on the surface of the Au core. This layer of CTAB may facilitate the deposition of incoming Au atoms on the Au–Ag alloy shell rather than on the Au core.

The thickness of the Ag shell is also a critical factor in the formation of uniform interior nanogaps. Fig. 2 shows the TEM images of NPs with interior nanogaps that were synthesized from Au–Ag core–shell NP templates with different thicknesses of the Ag shell. It is obvious that interior nanogaps only formed when the average thickness of the Ag shell was controlled to less than ~3.3 nm (Fig. S1, ESI† and Fig. 2b). Big and non-uniform gaps were detected inside NPs when the thickness of the Ag shell was larger than 5.0 nm (Fig. 2c and d). When $HAuCl_4$ reacted with the Ag shell, facets with higher surface energy started to corrupt and form pinholes. The galvanic reaction continued in the inner Ag shell until reaching the Au core, striping Ag^+ and electrons from the Ag shell. The electrons migrated to the surface of pitting sites and were then captured by $AuCl_4^-$, thus generating Au atoms that were deposited on the template. If the thickness of the Ag shell is larger than 5 nm, the Au core could move freely after the Ag shell was consumed by $HAuCl_4$, resulting in non-uniform and large gaps from the Au core to the alloy shell. While for the Au–Ag core–shell NPs with thinner shells ($< \sim 3.3$ nm), a small gap facilitated the formation of nanobridges between the shell and the Au core. The nanobridges provided support and prevented the movement of the Au core, leading to the formation of uniform nanogaps.

The size of interior gaps could be easily controlled by varying the thickness of the Ag shell template. Fig. 3 shows the STEM images of NPs with different sizes of interior nanogaps. The 2.5 nm nanogap was synthesized by Au–Ag core–shell NPs with a shell thickness of 3.3 nm (Fig. 3a). The nanobridge was formed between the Au core and the Au–Ag alloy shell. The reaction pathway for the formation of interior nanogaps is illustrated in Fig. S5 (ESI†). First, the galvanic

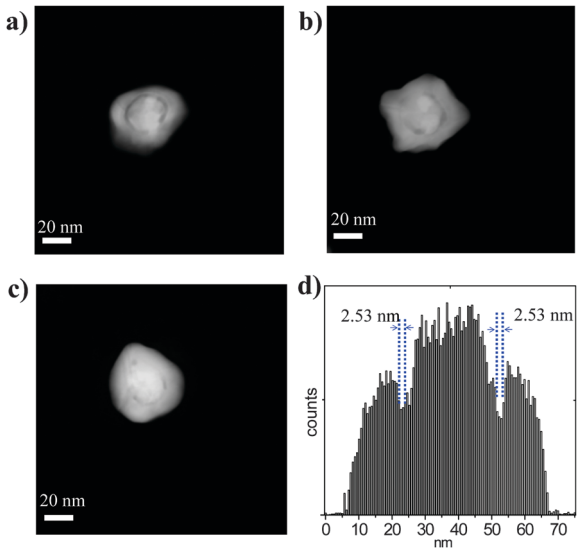

Fig. 3 STEM images of interior nanogaps with different sizes: (a) 2.5 nm, (b) 1.9 nm and (c) 0.9 nm; (d) EDS line scan.

reaction started at the pitting sites forming a thin layer as a template for subsequent deposition of Au atoms when $HAuCl_4$ was added to the Au–Ag NPs (Fig. S5a, ESI†). In galvanic reaction, Au atoms were continuously produced between the thin layer and the Au core and diffused to the outside direction. These Au atoms first came into contact with the thin layer template and preferentially nucleated on the inner side of the template. Meanwhile, Ag^+ was also reduced by ascorbic acid and thus formed the Au–Ag alloy on the template (Fig. S5b, ESI†). According to the stoichiometric relationship of $AuCl_4^-$ and Ag, only one gold atom is generated when every three silver atoms are oxidized. The resulting thin layer of alloy should be around one ninth of Ag thickness.[10] The size of the as-synthesized nanogaps was 2.5 nm instead of 3.3 nm. The same phenomenon is also observed for interior nanogaps with sizes of 1.9 and 0.9 nm (Fig. 3b and c). The size of nanogaps based on the thickness of the Ag shell is calculated to be ~2.9 nm, which is very close to the observed size of 2.5 nm. Herein, we added excess $HAuCl_4$ to fabricate interior nanogaps. Therefore, the sufficient supply of Au atoms reduced by ascorbic acid not only seamed the pitting holes and nucleated on the outside of the template (Fig. S5c, ESI†), but also enhanced the diffusion speed of Au atoms toward the inner Au core through the pinholes, thus generating bridges connecting the core and the alloy shell. The smaller the gap size, the more bridges formed between the core and the shell. As expected, the STEM images clearly show that the area of bridges increased with the decrease in nanogap size (Fig. 3a–c). We also carefully examined the presence of interior 2.5 nm nanogaps by energy dispersive spectroscopy (EDS). The line scanning of EDS was conducted on a typical NP with an interior nanogap and the response from Ag and Au was used to calculate the gap size. As shown in Fig. 3d, the response of EDS experienced a sudden decrease from 22.04 to 24.57 nm and from 51.67 to 54.20 nm, indicating a hollow space inside the NP. The gap size is calculated to be 2.53 nm based on the EDS profile, which confirms the results obtained from STEM. The elemental distribution of Ag and Au in NPs was also calculated according to the EDS line scan (Fig. S6, ESI†). A maximum percentage of Ag was observed close to the gap position. It is worth noting that there are some solid areas bridging the core and the shell. The bridge can be observed in the STEM images as the white area between the core and the shell. The elemental mapping of Au and Ag also clearly shows that the formation of the Au–Ag alloy shell was initiated on the edge of the template (Fig. S7, ESI†). In addition, it was found that the electromagnetic field of the nanogap was much more intense than that of a single nanoparticle (Fig. S8, ESI†). The Au core and the Au or the Ag shell with nanogaps have been used by several research groups and large enhancement of Raman signals has been observed due to enormous electromagnetic field in the nanogap.[5a,11]

In summary, a facile method was developed to fabricate Au–Ag core–shell nanoparticles with uniform nanogaps in controllable sub-2.5 nm size. This was based on the galvanic reaction of Ag and $HAuCl_4$ in the presence of CTAB. The success of this controlled synthesis could be attributed to fast dissolution of AgCl and AgBr in CTAB solution, which allowed the crystal growth of the shell on a designed template without interference from AgCl and AgBr. The thickness of the Ag shell is also a critical factor in the formation of uniform nanogaps. Bridged nanogaps were formed between the Au core and the Au–Ag shell when the average shell thickness was less than ~3.3 nm. Furthermore, the size of nanogaps (0.9–2.5 nm) could be easily controlled by varying the thickness of the Ag shell of the Au–Ag core–shell precursor. This approach is a simple and economic route to synthesize a new class of nanostructures with controllable interior nanogaps. The proposed method might also serve as a new method to create uniform nanogaps in other types of nanostructures.

Notes and references

1 (*a*) X. Qian, X. H. Peng, D. O. Ansari, Q. Yin-Goen, G. Z. Chen, D. M. Shin, L. Yang, A. N. Young, M. D. Wang and S. Nie, *Nat. Biotechnol.*, 2008, **26**, 83–90; (*b*) A. Schroeder, D. A. Heller, M. M. Winslow, J. E. Dahlman, G. W. Pratt, R. Langer, T. Jacks and D. G. Anderson, *Nat. Rev. Cancer*, 2011, **12**, 39–50; (*c*) M. S. Yavuz, Y. Cheng, J. Chen, C. M. Cobley, Q. Zhang, M. Rycenga, J. Xie, C. Kim, K. H. Song and A. G. Schwartz, *Nat. Mater.*, 2009, **8**, 935–939; (*d*) D.-K. Lim, I.-J. Kim and J.-M. Nam, *Chem. Commun.*, 2008, 5312–5314.
2 (*a*) X. M. Lin, Y. Cui, Y. H. Xu, B. Ren and Z. Q. Tian, *Anal. Bioanal. Chem.*, 2009, **394**, 1729–1745; (*b*) J. N. Anker, W. P. Hall, O. Lyandres, N. C. Shah, J. Zhao and R. P. Van Duyne, *Nat. Mater.*, 2008, **7**, 442–453.
3 (*a*) D. K. Lim, K. S. Jeon, H. M. Kim, J. M. Nam and Y. D. Suh, *Nat. Mater.*, 2009, **9**, 60–67; (*b*) S. Li, M. a. L. Pedano, S.-H. Chang, C. A. Mirkin and G. C. Schatz, *Nano Lett.*, 2010, **10**, 1722–1727; (*c*) Y. Fang, N.-H. Seong and D. D. Dlott, *Science*, 2008, **321**, 388–392; (*d*) G. Chen, Y. Wang, M. Yang, J. Xu, S. J. Goh, M. Pan and H. Chen, *J. Am. Chem. Soc.*, 2010, **132**, 3644–3645.
4 (*a*) K. Sato, K. Hosokawa and M. Maeda, *J. Am. Chem. Soc.*, 2003, **125**, 8102–8103; (*b*) R. Kanjanawarut and X. Su, *Anal. Chem.*, 2009, **81**, 6122–6129; (*c*) L. Sun, C. Yu and J. Irudayaraj, *Anal. Chem.*, 2007, **79**, 3981–3988; (*d*) D.-K. Lim, K.-S. Jeon, H. M. Kim, J.-M. Nam and Y. D. Suh, *Nat. Mater.*, 2010, **9**, 60–67.
5 (*a*) D. K. Lim, K. S. Jeon, J. H. Hwang, H. Kim, S. Kwon, Y. D. Suh and J. M. Nam, *Nat. Nanotechnol.*, 2011, **6**, 452–460; (*b*) W. Li, P. H. C. Camargo, X. Lu and Y. Xia, *Nano Lett.*, 2008, **9**, 485–490; (*c*) S. Y. Lee, L. Hung, G. S. Lang, J. E. Cornett, I. D. Mayergoyz and O. Rabin, *ACS Nano*, 2010, **4**, 5763–5772.
6 H. Im, K. C. Bantz, N. C. Lindquist, C. L. Haynes and S.-H. Oh, *Nano Lett.*, 2010, **10**, 2231–2236.
7 G. Frens, *Nature*, 1973, **241**, 20–22.
8 B. Liu, G. Han, Z. Zhang, R. Liu, C. Jiang, S. Wang and M. Y. Han, *Anal. Chem.*, 2012, **84**, 255–261.
9 E. Gonzalez, J. Arbiol and V. F. Puntes, *Science*, 2011, **334**, 1377–1380.
10 Y. Sun, B. Mayers and Y. Xia, *Adv. Mater.*, 2003, **15**, 641–646.
11 (*a*) N. Gandra and S. Singamaneni, *Adv. Mater.*, 2012; (*b*) N. Gandra, C. Portz and S. Singamaneni, *Nanoscale*, 2013, **5**, 1806–1809.